AD-A176 593 CW AND TRANSIENT MULTIRESONANT STUDIES IN THE NEAR MILLIMETER WAVE SPECTRUM(U) DUKE UNIV DURHAM NC DEPT OF PHYSICS D D SKATRUD 15 DEC 86 ARO-24015.2-PH 1/1

UNCLASSIFIED DAAL03-86-C-0011 F/G 20/5 NL

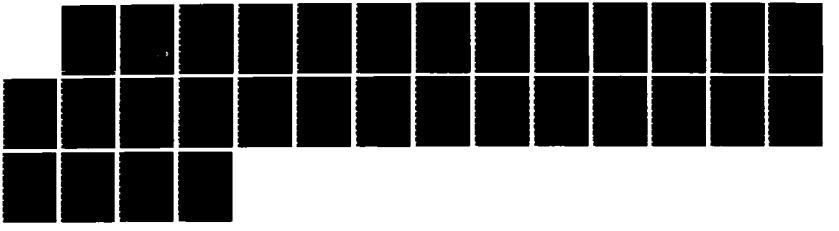

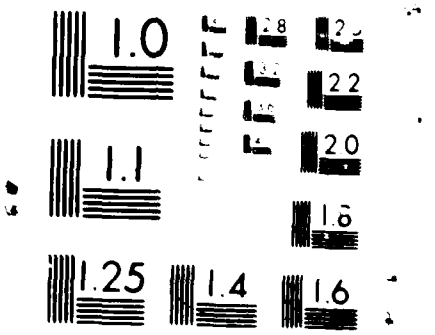
1.0
1.1
1.25
1.4
1.6
2.2
2.0
1.8

CW AND TRANSIENT MULTIRESONANT STUDIES IN THE NEAR MILLIMETER WAVE SPECTRUM

FINAL REPORT

David D. Skatrud

15 December 1986

U.S. ARMY RESEARCH OFFICE

Contract Number: DAAL03-86-C-0011

Duke University

APPROVED FOR PUBLIC RELEASE;
DISTRIBUTION UNLIMITED

MASTER COPY - FOR REPRODUCTION PURPOSES

UNCLASSIFIED
SECURITY CLASSIFICATION OF THIS PAGE (When Data Entered)

REPORT DOCUMENTATION PAGE		READ INSTRUCTIONS BEFORE COMPLETING FORM
1. REPORT NUMBER: ARO 24015.2-PH	2. GOVT ACCESSION NO.: N/A	3. RECIPIENT'S CATALOG NUMBER: N/A
4. TITLE (and Subtitle): CW AND TRANSIENT MULTIRESONANT STUDIES OF THE NEAR MILLIMETER WAVE SPECTRUM		5. TYPE OF REPORT & PERIOD COVERED: FINAL REPORT 1 Apr 1986 - 30 Sep 86
		6. PERFORMING ORG. REPORT NUMBER
7. AUTHOR(s): David Skatrud		8. CONTRACT OR GRANT NUMBER(s): DAAL03-86-C-0011
9. PERFORMING ORGANIZATION NAME AND ADDRESS: Department of Physics, Duke University, Durham, NC 27705		10. PROGRAM ELEMENT, PROJECT, TASK AREA & WORK UNIT NUMBERS
11. CONTROLLING OFFICE NAME AND ADDRESS: U. S. Army Research Office, Post Office Box 12211, Research Triangle Park, NC 27709		12. REPORT DATE: 15 Dec 1986
		13. NUMBER OF PAGES: 28
14. MONITORING AGENCY NAME & ADDRESS (if different from Controlling Office)		15. SECURITY CLASS. (of this report): Unclassified
		15a. DECLASSIFICATION/DOWNGRADING SCHEDULE

16. DISTRIBUTION STATEMENT (of this Report)

Approved for public release; distribution unlimited.

17. DISTRIBUTION STATEMENT (of the abstract entered in Block 20, if different from Report)

NA

18. SUPPLEMENTARY NOTES

The view, opinions, and/or findings contained in this report are those of the author(s) and should not be construed as an official Department of the Army position, policy, or decision, unless so designated by other documentation.

19. KEY WORDS (Continue on reverse side if necessary and identify by block number)

Near millimeter spectrum, far-infrared lasers, cw and transient multiresonance, molecular energy transfer

20. ABSTRACT (Continue on reverse side if necessary and identify by block number)

Several complimentary techniques have been used to study and develop gas phase quantum electronic systems in the near millimeter wave region of the spectrum. These techniques include cw transient and multiresonant experiments on optically pumped far-infrared lasers. In addition, modeling of our recently developed ultra-small lasers has demonstrated the importance of a previously ignored energy transfer mechanism. This mechanism is the vibrational-vibrational exitation of other excited vibrational states and it allows lasing at significantly higher pressures and smaller cell diameters than was previously assumed to be possible.

DD FORM 1 JAN 73 1473 EDITION OF 1 NOV 65 IS OBSOLETE

UNCLASSIFIED
SECURITY CLASSIFICATION OF THIS PAGE (When Data Entered)

TABLE OF CONTENTS

I. STATEMENT OF PROBLEM STUDIED

The objective of this study has been to advance the state of the knowledge about fundamental energy transfer mechanisms effecting vibrational and rotational energy distributions in low pressure molecular gases. The emphasis has been on mechanisms and parameters that impact the operation of optically pumped far-infrared (OPFIR) laser systems. Both cw and transient experiments were performed. Under cw conditions, measurements such as high precision line frequencies and pressure broadening parameters were obtained. For transient experiments a Q-switched CO_2 laser was used to induce nonequilibrium population distributions; the subsequent population flow was then monitored by means of our millimeter/submillimeter rotational spectroscopic techniques. This allows the determination of the cross sections and rates for specific energy transfer processes. The results of these experiments were incorporated in a computer simulation that has been used to model OPFIR lasers. This model was also shown to correctly predict the behavior of our recently developed ultra-small OPFIR lasers which operate outside of the bounds allowed under previously accepted theory.

II. SUMMARY OF THE MOST IMPORTANT RESULTS

We have completed an extensive spectroscopic study of the OPFIR laser molecule $^{12}CH_3F$. We have measured a large number of pure rotational transition frequencies in both the ground vibrational state and also in the excited vibrational state containing the laser transitions. These measurements include the laser transitions themselves. In addition, we have measured pressure broadening parameters for a number of these transitions. The measured transition frequencies have been used in a fit to the well known model for symetric top molecules. The resulting predicted frequencies are accurate to 10 kHz at 300 GHz; which is better than a part in 3×10^7. More details on this experiment, data, and results are contained in the appendix starting on page 4. This appendix contains excerpts from a joint paper with Dr. Richard Schwendeman's group at Michigan State University. In this paper our pure rotational measurements have been combined with their vibrational measurements.

We have also obtained significant results in our transient multiresonant study of the $^{13}CH_3F$ OPFIR laser system. These measurements have allowed us to differentiate among collisions that change the energy of the molecule due to the angular momentum, the projection of the angular

momentum, and the vibrational states (designated J, K, and v, respectively). A computer simulation guided by the results of these experiments then allows for the quantification of the rates for these processes. The K changing rate was found to be equal to the rapid J changing rate (which is approximately ten times the gas kinetic rate!). This surprising result can be explained by a swapping mechanism where the molecule changes vibrational quantum with ground state molecules.

The computer model has been used to explain the operation of our recently developed ultra-small OPFIR lasers. These lasers are about 10^4 times smaller and operate at pressures up to 100 times greater than standard OPFIR lasers. Previously accepted theory of OPFIR lasers had predicted a cut-off pressure beyond which the lasers would not oscillate; however, our lasers operate at a pressure more than an order of magnitude beyond this. We have shown that the mistake made by the others was the neglect of the effect other excited vibrational states. These vibrational states can actually end up with a significant portion of the pumped population by means of rapid vibrational vibrational exchange. The net result to to reduce the bottleneck in the lasing state and allow lasing to much higher pressures. A detailed explanation of this mechanism and its implications is contained in the appendix starting with page A1.

III. SCIENTIFIC PERSONNEL SUPPORTED BY THIS CONTRACT

David D. Skatrud

IV. LIST OF PUBLICATIONS AND PRESENTATIONS

A. Publications

1. Henry O. Everitt, David D. Skatrud, and Frank C. De Lucia, "Dynamics and tunability of a small optically pumped cw far-infrared laser" Appl. Phys. Lett. **49** 20, 20 Oct 86.

2. Sang K. Lee, R. H. Schwendeman, Richard L. Crownover, David D. Skatrud, and

Frank C. De Lucia, "Study of the ν_3 and $2\nu_3 \leftarrow \nu_3$ Bands of $^{12}CH_3F$ by Infrared Laser Sideband and Submillimeter Wave Spectroscopy" submitted to the J. Mol. Spec.

B. Presentations

1. Richard L. Crownover, David D. Skatrud, K.V.L.N. Sastry, and Frank C. De Lucia, "Frequency Measurements of FIR Lasing Transitions" paper TA9, 41st Symposium on Molecular spectroscopy, Ohio State University, Columbus, Ohio, June 16-20, 1986.

2. Rodney I. McCormick, David D. Skatrud, and Frank C. De Lucia, "Time Resolved Rotational Energy Transfer in $^{13}CH_3F$" paper RG2, 41st Symposium on Molecular spectroscopy, Ohio State University, Columbus, Ohio, June 16-20, 1986.

Dynamics and tunability of a small optically pumped cw far-infrared laser

Henry O. Everitt, David D. Skatrud,[a] and Frank C. DeLucia
Department of Physics, Duke University, Durham, North Carolina 27706

(Received 17 July 1986; accepted for publication 25 August 1986)

We report the development of an ultrasmall, optically pumped cw far-infrared (FIR) laser that provides substantial tunability. This laser operates at pressures significantly higher than the maximum allowed by currently accepted theory. We also report the development of a new theoretical model for diffusion limited optically pumped FIR lasers which accounts for this behavior. It is shown that the consideration of additional higher energy vibrational states, along with appropriate energy transfer mechanisms, fundamentally alters the behavior of the system in the high pressure, high pump intensity regime. Although $^{13}CH_3F$ is used for both the experimental demonstration and the theoretical model, the concept is general and should apply to all diffusion relaxed FIR lasers.

It has been argued that the introduction of the optically pumped far-infrared (FIR) laser has done more to heighten activity in this spectral region than any other single development.[1] This has resulted from several factors, but chief among them has been their ease of construction, relatively low cost, and large number of available frequencies. One principal drawback of these lasers has been their lack of tunability. This is a direct consequence of their operation at low pressure, a requirement seemingly imposed on cw systems by rather fundamental theoretical considerations.[1-3]

For the large majority of optically pumped FIR lasers, whose vibrational relaxation is via diffusion to the walls, conventional models predict a maximum pressure beyond which no inversion can exist, independent of pump power. At high pump intensities the essence of the physics is that near the cut-off pressure two processes are both proportional to pump intensity. The first of these is the absorption due to the thermal population that builds up in the excited vibrational state as it diffuses to its relaxation at the wall. The second is the pump induced nonequilibrium gain. Detailed calculations lead to[1,2]

$$P_c = \left(\frac{K_d/K_c}{(g_u/g_l)f_l - f_u}\right)^{1/2}\left(\frac{1}{d}\right), \tag{1}$$

where P_c is the cut-off pressure, g_u the degeneracy of the upper laser state, g_l the degeneracy of the lower laser state, f_u the fractional occupation number of the upper laser state, and f_l the fractional occupation number of the lower laser state. K_d and K_c are defined by the diffusion vibrational relaxation rate $K_d P d^2$ and the rotational relaxation rate $K_c P$, respectively. This gives a cut-off pressure for the diffusion limited $^{13}CH_3F$ laser of $200/d$ mTorr, where d is the diameter of the cell in centimeters.

To understand the operation of our laser at pressures significantly above the "cut-off" pressure, the effects of vibrational states lying above the pumped state must be considered. For $^{13}CH_3F$ it is the $J = 5$, $K = 3$ rotational state in v_3 that is pumped from $J = 4$, $K = 3$ in the ground state by the $9P(32)$ CO_2 laser line. Although the details for a particular molecule may be complicated, the basic mechanism that breaks the vibrational bottleneck is straightforward. In the strong pump limit, the conventional model predicts the populations of the ground and pumped excited vibrational state approach equality. It implicitly assumes that the higher lying vibrational states maintain their original negligible populations and do not actively participate in the laser operation. However, because vibrational energy transfer processes such as

$$CH_3F(v_3 = 1) + CH_3F(v_3 = 1) \rightarrow CH_3F(v_3 = 2) + CH_3F(v_3 = 0) + \Delta E \tag{2}$$

have very small energy defects ΔE, they can be highly probable[4] and significant numbers of molecules will be promoted to these higher lying states. Consequently, all states within the particular mode will have essentially the same vibrational temperature. In addition, a multitude of similar resonant or near resonant processes couple other vibrational modes, thereby establishing nearly the same vibrational temperature among all states.

This leads to two effects, both of which significantly alter the predictions of the conventional model in the high pump, high pressure regime. First, the growth of population in this extended vibrational pool decreases the thermal absorption that must be overcome by the nonthermal gain and effectively changes the definitions of f_l and f_u in Eq. (1). Second, each time a more highly excited molecule relaxes at the wall several additional molecules have also decayed via the resonant molecule-molecule process that produced it. For example, the relaxation of a $2v_3$ molecule involves the decay of two molecules to the ground state, one from the creation of the $2v_3$ molecule via Eq. (2), the other from the diffusion of the $2v_3$ molecule itself. Thus, the effective vibrational relaxation rate is faster than the diffusion rate. *Since the size of the extended vibrational pool grows without bound with increasing pump intensity, both of these effects eliminate an absolute vibrational bottleneck.*

For the experimental work, two copper laser cavities were used, one with a diameter of 0.5 cm and a length of 15.0 cm, the other with dimensions of 0.25 cm by 5.0 cm. The length was adjusted by a translatable mirror insert, and both input and output were coupled through a 1.0-mm-diam hole in the other end. The smaller cavity had a volume $\sim 10^{-4}$ of that occupied by a typical FIR laser, and operated to pressure 10–100 times higher. It should be noted that a number of parameters such as cavity Q, cavity size, and pump coupling were not optimized in this initial work. Figure 1 shows

[a] Current address: Army Research Office, P. O. Box 12211, Research Triangle Park, NC 27709.

A1

 0003-6951/86/420995-03$01.00

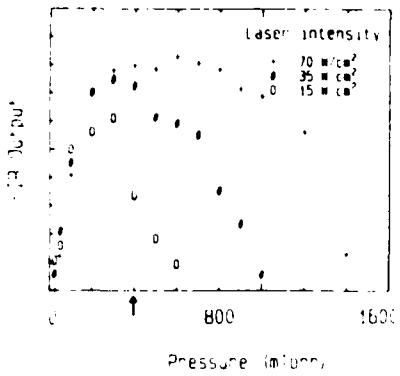

FIG. 1. Output power in arbitrary units of the 0.5 cm × 15.0 cm FIR laser measured as a function of incident pump laser intensity and pressure. The arrow at 400 mTorr shows the cut-off pressure as calculated from the conventional model.

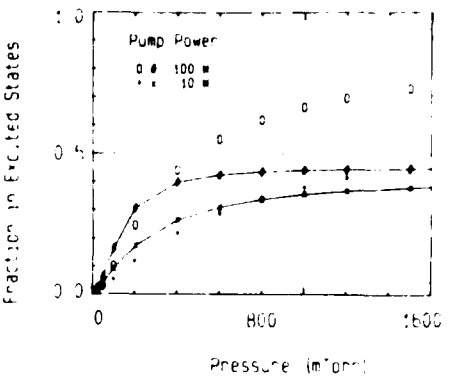

FIG. 2. Fraction of molecules in excited vibrational states as a function of pressure for two circulating pump powers. The connected points are the predictions of conventional theory while the unconnected points correspond to extended theory.

the power output of the larger laser as a function of pressure and incident pump intensity for an experimental run with $^{13}CH_3F$ as the laser medium. This figure directly illustrates the experimentally observed absence of a pressure limit on the operation of this laser. Also, we observed no evidence that the maximum lasing pressure could not be increased if a stronger pump were available. It is important to note that this experiment was in the high pump intensity limit because of the small diameter of the laser cavity, not because a particularly powerful CO_2 pump laser was used. Although accurate FIR power measurements were not attempted, estimates based on the noise equivalent power (NEP) of the Golay detector used in the experiment indicate powers of about 0.1 mW were obtained. Scaling arguments based on cavity size, pressure, and pump absorption show that output powers approaching those of standard large cell cw lasers may be obtained by more careful cavity design and optimizations.

We have previously undertaken a series of experiments in which millimeter and submillimeter wave spectroscopy was used as a diagnostic probe to observe the internal dynamics of FIR laser operating in the conventional pressure and pump intensity regime. We also discussed a model that accounts for the details of rotational collisional processes that are significant in that regime.[5-7] This model was used as a starting point for our extended model which is valid for lasers operating in the high pressure, high pump intensity regime as well. In this numerical simulation, the 31 vibrational states lying below 3300 cm^{-1} were included. The population and associated energy pumped into v_3 were distributed among all these vibrational states as determined by the assumption of a single vibrational temperature. This assumption is a good approximation in diffusion limited lasers since the vibrational exchange mechanisms such as Eq. (2) are much faster than the competing processes. The details of the implementation of this model will be published elsewhere.

The effects of the inclusion of the extended vibrational pool can best be appreciated from comparisons of several predictions of the two models. Figure 2 shows the fraction of molecules in excited vibrational states for both the conventional and extended models. As expected, the conventional model curves approach 0.5 at high pressure. However, in the extended model the fraction approaches 1.0, and a larger dependence on pump power is also noted. Figure 3 shows the vibrational temperature (calculated between the ground state and v_3) as a function of pressure and pump intensity. It can be seen that without the extended vibrational pool, the temperature increases rapidly, whereas with the extended vibrational pool the ever increasing heat capacity of the system causes the temperature to rise much more slowly. Figure 4 shows the predicted population inversion of the laser as a function of pressure and circulating pump power. Under strong pump conditions, the extended model predicts that lasing in the ground vibrational state can exist at pressures at least as high as those for the excited vibrational state lasing. Since most of our measurements were not made with frequency selective (i.e., heterodyne) techniques, the observed output power from the two states could not be distinguished. However, in our heterodyne experiments, we have observed ground state lasing that seems to confirm this prediction. As can be seen, there is good agreement with the experimental results for the dependence of the maximum lasing pressure on pump power, whereas models without the extended vibrational pool predict a vibrational bottleneck induced cutoff. Since we have been primarily interested in the high pressure regime, our model does not currently include the effects

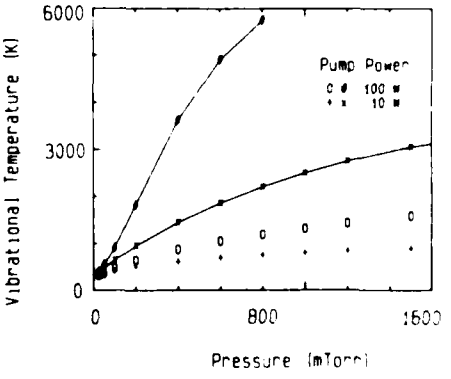

FIG. 3. Vibrational temperature as a function of pressure for two circulating pump powers. The connected points are the predictions of conventional theory while the unconnected points correspond to extended theory.

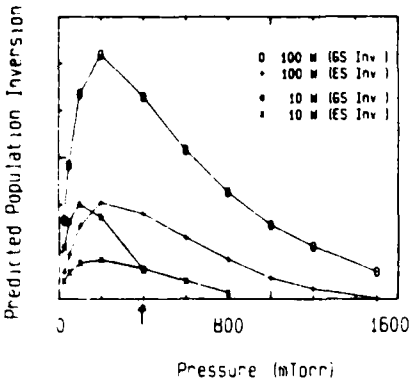

FIG. 4. Predicted laser population inversion as a function of circulating pump power and pressure for both the ground and excited vibrational states. The arrow at 400 mTorr shows the cut-off pressure predicted by conventional theory.

of hole burning. This causes the calculated inversions to be too large at low pressure.

For a laser operating at 400 mTorr, we have directly measured a tunability of 24 MHz with heterodyne techniques. Since we have operated this laser to ~3 Torr pressure and its linewidth parameter is ~40 MHz/Torr [full width half-maximum (FWHM)], we conclude that its tunability is ~100 MHz. Although we have not made a detailed investigation of the spectral purity of the laser, the beat notes that result from the heterodyne experiments appear to be similar to the high spectral purity beat notes observed between low pressure FIR lasers and tunable electronic sources.

We have used the extended model to calculate the maximum pressure of operation for the $^{13}CH_3F$ laser in fundamental waveguide. With 100 W of circulating pump power, it predicts inversion to ~25 Torr which corresponds to a tunability of about 1 GHz. Since the current model only includes vibrational states of energy $< 3300\ cm^{-1}$ and assumes a relatively low circulating pump power, this may be a conservative estimate. This tunability would still be substantially less than is available from Raman tuned FIR lasers.[8,9] However, since Raman tuned lasers require pulsed operation with multi-atmosphere transverse, electric, atmospheric lasers, the cw operation of the small lasers would offer significant advantages for some applications. Although the peak powers of Raman tuned lasers are $\sim 10^7$ times larger than those of our small lasers (the average powers are about equal), the peak spectral intensity of the small lasers is equal to or larger than those of the Raman tuned lasers.

It will be interesting to consider the optimization of cavity parameters in this regime and to extend this work both experimentally and theoretically to other species. Because of the significantly higher pressure and pump intensity of our small lasers, it may well be that the best species and transitions for them are different from the best for conventional lasers. For example, the increased bandwidth of the IR absorption line at high pressure significantly reduces the pump absorption coincidence requirement.

In summary, we have demonstrated the operation of a small, tunable FIR laser in a pressure regime higher than previously believed possible. We have also shown how the inclusion of more highly excited vibrational states omitted in the conventional model accounts for its operation. It would appear that the newly described process is very general and should make possible the construction of many FIR lasers whose absolute tunability is at least as good as that of tunable waveguide CO_2 lasers and whose relative tunability is 100 times larger.

This research was supported by the U. S. Army Research Office contract DAAG-29-83-K-0078 and instrumentation grant DAAG-29-83-G-0047.

[1] M. S. Tobin, Proc. IEEE **73**, 61 (1985).
[2] D. T. Hodges, J. R. Tucker, and T. S. Hartwick, Infrared Phys. **16**, 175 (1976).
[3] T. A. DeTemple and E. J. Danielwicz, IEEE J. Quantum Electron. **QE-12**, 40 (1976).
[4] G. W. Flynn and E. Weitz, J. Chem. Phys. **58**, 2781 (1973).
[5] W. H. Matteson and F. C. DeLucia, IEEE J. Quantum Electron. **QE-19**, 1284 (1983).
[6] W. H. Matteson and F. C. DeLucia, J. Opt. Soc. Am. B **2**, 336 (1985).
[7] R. I. McCormick, D. D. Skatrud, and F. C. DeLucia, 41st Symposium on Molecular Spectroscopy, The Ohio State University, Columbus, Ohio, 1986.
[8] S. J. Petuchowski, A. T. Rosenberger, and T. A. DeTemple, IEEE J. Quantum Electron. **QE-13**, 476 (1977).
[9] B. G. Danly, S. G. Evangelides, R. J. Temkin, and B. Lax, IEEE J. Quantum Electron. **QE-20**, 834 (1984).

Study of the ν_3 and $2\nu_3 \leftarrow \nu_3$ Bands of $^{12}CH_3F$ by Infrared Laser Sideband and Submillimeter Wave Spectroscopy[a]

Sang K. Lee[b] and R. H. Schwendeman
Department of Chemistry
Michigan State University
East Lansing, MI 48824

Richard L. Crownover, David D. Skatrud[c], and Frank C. De Lucia
Department of Physics
Duke University
Durham, NC 27706

[a] This material is based on work partially supported at MSU by the National Science Foundation under Grant No. 83-12861 and at Duke University by the U.S. Army Research Office under Contract No. DAAG-29-83-K-0078 and DAAL03-86-C-0011.

[b] Current Address: Herzberg Institute of Astrophysics, National Research Council of Canada, Ottawa, Ontario K1A OR6.

[c] Current Address: Army Research Office, P.O. Box 12211, Research Triangle Park, NC 27709.

Abstract

An infrared laser sideband spectrometer operating in the CO_2 laser region with 8-18 GHz sidebands has been used to record 266 transitions in the ν_3 band and 84 transitions in the $2\nu_3 \leftarrow \nu_3$ band of $^{12}CH_3F$. The accuracy of the measured frequencies is estimated to be 1-3 MHz. A millimeter/submillimeter wave spectrometer has been used to record the spectra of 48 pure rotational transitions in the ground vibrational state and 55 transitions in the $v_3 = 1$ vibrational state with an accuracy of 20-90 kHz. The new measurements have been combined with previous radio frequency and infrared laser results to derive sets of constants for the ground, $v_3 = 1$, and $v_3 = 2$ states for this molecule. Tables of the vibrational dependence of the parameters and of the near coincidences of the ν_3 and $2\nu_3 \leftarrow \nu_3$ band transitions with CO_2 laser frequencies are given.

I. Introduction

Recently, portions of the ν_3 and $2\nu_3 \leftarrow \nu_3$ bands of $^{13}CH_3F$ were recorded at Michigan State University (MSU) by means of an infrared microwave sideband laser spectrometer (1). In order to assign the weak hot band transitions unambiguously, it proved necessary to measure the ν_3 spectrum of $^{12}CH_3F$, since the sample of $^{13}CH_3F$ used was not entirely free of the parent species. Because there have been a large number of recent high resolution studies of the ν_3 band of $^{12}CH_3F$ (2-5), we had expected to be able to calculate the frequencies to within 10-20 MHz with available constants, even for rather high J. It turned out, however, that for $J > 20$, particularly for P-branch transitions, the deviation between observed and calculated frequencies was rather sizeable, reaching more than 200 MHz (0.007 cm^{-1}).

Since the method of infrared-microwave sideband laser spectroscopy, as developed by Mageri and his coworkers (6), and applied to several spectroscopic studies (1,7-15), can easily provide frequencies of spectra that are accurate to a few MHz, we decided to extend the study of the ν_3 band of $^{12}CH_3F$ to as many transitions as could be measured in the range of our spectrometer and also to record as much of the spectrum of the $2\nu_3 \leftarrow \nu_3$ band as possible. The analysis of the ν_3 band of $^{12}CH_3F$ has been discussed in detail many times (2-5) and the present analysis is very similar to the previous study of $^{13}CH_3F$ (1). We will therefore simply present the spectra and the resulting parameters and only briefly describe the experimental and theoretical details.

As part of a study at Duke University of the dynamics of far infrared laser action in $^{12}CH_3F$ it was necessary to monitor the absorption of pure rotational transitions in the ground and $\nu_3 = 1$ vibrational states of this

molecule. The millimeter wave spectra of these transitions were at the time limited to relatively low J and K (16-19); therefore, the first step in this study was to measure the frequencies of a large number of rotational transitions in both vibrational states. Since these measurements were made, a report of millimeter and submillimeter wave frequencies for the ground vibrational state for the same J range and K = 0, 3, 6, etc. has appeared (20). Comparison of the results of these measurements with the values reported here is given below. In addition to the work already cited, rotation or vibration rotation frequencies for the ground and $v_3 = 1$ states or for the v_3 band have been measured by combination differences of Fourier transform spectra (21), IR-RF two-photon spectroscopy (22), diode laser spectroscopy (23-24), waveguide laser spectroscopy (24), and optical pumping (25-28).

In the present paper, Section II is a description of the experimental techniques used to record and measure the infrared, millimeter wave, and submillimeter wave frequencies. Section III describes the energy level expressions used to calculate the spectra, Section IV presents the results of least-squares fitting of the spectra, and Section V summarizes the results.

II. Experiment

The infrared microwave sideband laser spectrometer at MSU has been described in previous publications (1,14) and therefore only a brief description will be given here. Infrared radiation (~0.5 W) from a frequency-stabilized CO_2 laser is focused onto a CdTe electro-optic crystal that is simultaneously irradiated by high power (~10 W, 8-18 GHz) microwaves. The infrared carrier and microwave-generated sidebands are recollimated and passed through a polarizer that removes most of the carrier. The microwave radiation

is chopped at 33.3 kHz by a PIN diode absorptive modulator before being applied to the sideband generator. For the present study, a feedback circuit controlled the amplitude of the applied microwaves during the "on" period of the PIN diode to maintain constant sideband power. With this system it is possible to sweep over 2-3 GHz (0.067 - 0.1 cm^{-1}) with the infrared amplitude at a reference detector held constant to within a few tenths of one per cent. Fig. 1 is a block diagram of the spectrometer showing the location of the leveling circuit and the PIN diode. The infrared sidebands are passed through a sample cell to a detector whose output is processed at 33.3 kHz by a lock-in amplifier. A minicomputer steps the microwave frequency and records the output of the lock-in amplifier that monitors the sample beam detector and the nearly constant output of a similar system for the reference beam.

The sample cells are simple glass tubes with NaCl windows. The path length was 1 m and the sample pressures, as measured by a capacitance manometer, were < 200 mTorr for the fundamental band and < 1 Torr for the hot band. The $^{12}CH_3F$ sample used at MSU was obtained from Peninsular Chemical Research, Inc., and used as received. Composites of typical spectra are shown in Figs. 2 and 3. These spectra are reprinted as recorded from the spectrometer with no division by a reference spectrum. The flat background demonstrates the effectiveness of the amplitude leveling system.

The recorded spectra were fit to a Gaussian line shape as a function of microwave frequency. The infrared frequency of each transition was taken to be $\nu_\ell \pm \nu_m$, where ν_ℓ is the known laser frequency and ν_m is the center frequency of the Gaussian function. Since the spectra were rather well characterized prior to this work, the proper sign was usually known. In questionable cases the usual spectrum recorded with the infrared laser stabilized to the Lamb dip

in the fluorescence from an intracavity cell filled with CO_2 was compared to a spectrum recorded with the laser stabilized to one or another of the shoulders of the Lamb dip. The difference in the microwave frequencies of the two spectra provided an unambiguous choice of the sign in $\nu_\ell \pm \nu_m$. The overall accuracy of the individual spectral frequencies was estimated to be 1-3 MHz depending on the strength of the transition, the degree of overlapping, and the quality of the spectra in the given spectral region.

The pure rotational transitions were measured on a millimeter/submillimeter (mm/submm) wave spectrometer that has been developed at Duke University (29). This system provides continuous coverage from less than 100 GHz to greater than 1000 GHz with adequate sensitivity for room temperature absorption measurements in even highly excited vibrational states and transient species. Figure 4 shows a block diagram of the experimental apparatus. The mm/submm power is produced by a refined version of the crossed-waveguide crystal harmonic generator developed by King and Gordy (30). The multiplier is driven by an ~300 mW reflex klystron operating in the 55 GHz region. The output of the multiplier, after lower harmonics are removed by a waveguide-beyond-cutoff filter, is focused in to a sample cell and then directed onto a 1.5 K InSb hot-electron bolometer. The sample cell is a copper pipe 1 m in length by 1.25 cm in diameter. The klystron is phase-locked to a harmonic of a microprocessor controlled frequency synthesizer capable of phase continuous sweeps and simultaneous phase modulation. The data were typically acquired in segments that covered about 30 MHz with sweep times of 10 s. The signal was phase modulated at 1 kHz with lock-in detection at 2f and a time constant of 100 ms. Pairs of up/down frequency sweeps were averaged to cancel time-constant induced frequency shifts and other systematic errors. Additional

signal enhancement was obtained by digitally signal averaging the individual frequency sweeps. The net integration time for the weakest signals was about 10 minutes.

The frequency synthesizer is locked to a frequency standard which is in turn referenced to WWVB. The frequency of the mm/submm waves is thus known to an absolute accuracy of better than 10^9 and since the multiplier is driven by a reflex klystron, the spectral purity is high. Therefore, the observed linewidths were entirely due to the widths of the rotational transitions themselves. The sample pressure was adjusted to be small enough so that the dominant line-broadening mechanism was Doppler broadening which for CH_3F has a HWHM of $\Delta\nu = 10^{-6}\nu$. The typical pressure was ~30 mTorr, although lower pressures had to be used for many of the ground state transitions to prevent line broadening caused by near 100% absorption of the mm/submm wave power. The line centers were measured with an accuracy better than 5% of the HWHM by fitting a parabola to the peak of the absorptions. The 1σ uncertainty in the measurements was thus about 30 kHz (10^{-6} cm^{-1}) for transitions around 600 GHz.

The CH_3F sample used at Duke was obtained from Matheson Gas products. Figure 5 shows a typical absorption line, in this case the J=12←11, K=2 transition in the v_3=1 vibrational state. This is the strongest lasing transition in the CH_3F optically pumped far infrared laser (31). Although the absorptivities of the rotational transitions in the excited vibrational state are ~150 times smaller than in the ground state, a strong signal is still obtained with a reasonable integration time because of the large rotational absorption coefficients at these frequencies and the sensitivity of the system.

III. Theory

The spectral frequencies were fit to differences in energy levels given by the following expression

$$E(v,J,K) = \sum_{m,n=0}^{m+n=N} X_{mn}^{(v)} f^m g^n \qquad (1)$$

where $f = J(J+1)$, $g = K^2$, and the $X_{mn}^{(v)}$ are the usual vibration-rotation constants:

$$X_{00}^{(v)} = \text{vibrational energy},\ X_{10}^{(v)} = B_v,\ X_{01}^{(v)} = (A_v - B_v)\ ,$$

$$X_{20}^{(v)} = -D_J^{(v)},\ X_{11}^{(v)} = -D_{JK}^{(v)},\ X_{02}^{(v)} = -D_K^{(v)}\ ,$$

$$X_{30}^{(v)} = H_J,\ X_{40}^{(v)} = L_J,\ \text{etc.}$$

Since very good ground-state constants were available from the work of Graner (21), of Arimondo et al. (5), and of Poucher et al. (20), we extended our program to allow simultaneous fitting of the rotational frequencies in any level and of the frequencies of the fundamental and the hot band to obtain constants for $v_3 = 0$, 1, and 2 all at once, or to obtain constants with the $v = 0$ values constrained. In all of the least squares fittings the weight assigned to each experimental frequency was σ^{-2} where σ is the uncertainty in the measured value.

Since vibration-rotation parameters have been determined in this work for the $v_3 = 0$, 1, and 2 vibrational levels of $^{12}CH_3F$, it is possible to estimate the first three constants in an expansion of these parameters in powers of v_3. We used an expression of the form,

$$P(v) = P(0) + c_1 v + c_2 v^2 \qquad (2)$$

where P(v) is a parameter for the vibrational level v and c_1 and c_2 are constants.

The rotational levels of the $v_3 = 1$ (and presumably $v_3 = 2$) state of CH_3F are involved in a mild Coriolis resonance with the $v_6 = 1$ (and higher) levels. This resonance was ignored in the present work and the effects of the resonance are therefore included in the values of the parameters. The magnitude of these effects, which are substantial, have been estimated (4). In this reference it was shown that the standard deviation in the fit of spectra to rather high J and K is comparable for fits that include explicit consideration of the Coriolis coupling and those that ignore it. Consequently, in the absence of better constants for the $v_6 = 1$ and higher states, it is better for most purposes to ignore the resonance.

IV. Results

The frequencies of the vibration-rotation transitions observed in this work are given in Table I for the ν_3 fundamental band and in Table II for the $2\nu_3 + \nu_3$ hot band. The frequencies of the rotational transitions observed in this work are given in Table III for the ground vibrational state and in Table IV for the $v_3 = 1$ state. The sources of previously-reported experimental data that are included in the file of frequencies used in the least-squares fitting are summarized in Table V.

The frequencies in Tables I-IV together with those indicated in Table V have been used for a number of least-squares fits to energy levels calculated by means of Eq. (1). The vibration-rotation parameters obtained for a fit in

which all of the parameters for $N \leq 3$ for $v_3 = 0$ and $N \leq 4$ for $v_3 = 1$ and 2 were varied are given in Table VI. These parameters were used to calculate the values for the comparison of observed and calculated frequencies in Tables I-IV. In a second fitting, parameters were determined by constraining the ground state constants to those reported by Arimondo et al. (5), which were obtained from a fitting that included Graner's ground state combination differences (21). The constants from this fitting are in close agreement with those in Table VI. The reason for this may be seen in Table VII where the parameters for the ground state obtained from the fit in Table VI are compared to the corresponding parameters obtained by fitting only the data in Table III, and to the constants reported by Arimondo et al. (5) and by Boucher et al. (20). The ground state parameters obtained from our full fitting (I) are in very good agreement with those obtained from a variety of purely ground state data.

The vibrational dependence (Eq. (2)) of the constants calculated from the parameters in Table VI are shown in Table VIII, where the more usual notation for some of the parameters is indicated.

In Tables IX and X the calculated (parameters in Table VI) vibration-rotation frequencies for the ν_3 ($J \leq 40$, $K \leq 15$) and $2\nu_3 \leftarrow \nu_3$ ($J \leq 25$, $K \leq 12$) bands, respectively, that lie within 100 MHz of a CO_2 laser frequency are shown together with the calculated offset. The CO_2 parameters for this calculation were taken from Ref. (32-34).

V. Discussion

As indicated in the Introduction it was not possible with the parameters previously available for the ν_3 band to compute the frequencies for J - 20 to

an accuracy of 10-20 MHz. This situation, which appeared to be mainly the result of an insufficient number of precise P band frequencies, has been remedied. It should now be possible to compute the frequencies for $J \leq 30$, $K \leq 15$ for the ν_3 band and $J \leq 20$, $K \leq 10$ for the $2\nu_3 \leftarrow \nu_3$ band to an accuracy of ~ 5 MHz. In addition, it should be possible to calculate all of the rotational frequencies for $J \leq 20$ for $v_3 = 0$ and $J \leq 14$ for $v_3 = 1$ to ~ 80 kHz. In all cases the uncertainties rise rapidly with J and K and are much smaller for low J.

The overall standard deviation for an observation of unit weight for the 668 frequencies included in the full fitting was 1.3 MHz, which could be the result of a 30% underestimation of the experimental uncertainties, an inadequacy of the model used for the calculation, or some combination of these two effects. We believe that the discrepancy is mainly the result of model error. One indication that this might be so is that inclusion of L constants ($N = 4$ in Eq. 1) for the ground state rotational levels does not improve the fit significantly. By contrast, L constants are essential for $v_3 = 1$ and 2. This is probably a result of an attempt by the power series expansion (Eq. 1) to account for the Coriolis coupling to the ν_6 levels.

REFERENCES

1. S. K. Lee, R. H. Schwendeman, and G. Magerl, J. Mol. Spectrosc. 117, 416-434 (1986).

2. S. M. Freund, G. Duxbury, M. Romheld, J. T. Tiedje, and T. Oka, J. Mol. Spectrosc. 52, 38-57 (1974). M. Romheld, Ph.D. thesis, University of Ulm, 1979.

3. E. Arimondo and M. Inguscio, J. Mol. Spectrosc. 75, 81-86 (1979).

4. P. Shoja-Chaghervand and R. H. Schwendeman, J. Mol. Spectrosc. 98, 27-40 (1983).

5. E. Arimondo, M. I. Schisano, P. B. Davies, and P. A. Hamilton, Infrared Phys. 25, 209-213 (1985).

6. G. Magerl, W. Schupita, and E. Bonek, IEEE J. Quantum Electron. QE-18, 1214-1220 (1982).

7. G. Magerl, E. Bonek, and W. A. Kreiner, Chem. Phys. Lett. 52, 473-476 (1977).

8. G. Magerl, W. A. Kreiner, B. Furch, and E. Bonek, Acta Phys. Austriaca Suppl. 20, 167-179 (1979).

9. W. A. Kreiner, G. Magerl, B. Furch, and E. Bonek, J. Chem. Phys. 70, 5015-5020 (1979).

10. G. Magerl, W. Schupita, E. Bonek, and W. A. Kreiner, J. Chem. Phys. 72, 395-398 (1980).

11. G. Magerl, W. Schupita, E. Bonek, and W. A. Kreiner, J. Mol. Spectrosc. 83, 431-439 (1980).

12. G. Magerl, J. M. Frye, W. A. Kreiner, and T. Oka, Appl. Phys. Lett. 42, 656-658 (1983).

13. G. Magerl, W. Schupita, J. M. Frye, W. A. Kreiner, and T. Oka, J. Mol. Spectrosc. 107, 72-83 (1984).

14. H. Sasada, R. H. Schwendeman, G. Magerl, R. L. Poynter, and J. M. Margolis, J. Mol. Spectrosc. 117, 317-330 (1986).

15. H. Sasada and R. H. Schwendeman, J. Mol. Spectrosc. 117, 331-341 (1986).

16. R. S. Winton and W. Gordy, Phys. Lett. 32A, 219-220 (1970).

17. T. E. Sullivan and L. Frenkel, J. Mol. Spectrosc. 39, 185-201 (1971).

18. T. Tanaka and E. Hirota, J. Mol. Spectrosc. 54, 437-446 (1975).

19. E. Hirota, T. Tanaka, and S. Saito, J. Mol. Spectrosc. 63, 478-484 (1976).

20. D. Boucher, J. Burie, R. Bocquet, and J. Demaison, J. Mol. Spectrosc. 116, 256-258 (1986).

21. G. Graner, Mol. Phys. 31, 1833-1843 (1976).

22. S. M. Freund, M. Romheld, and T. Oka, Phys. Rev. Lett. 35, 1497-1500 (1975).

23. J. P. Sattler and G. J. Simonis, IEEE J. Quantum Electron. QE-13, 461-465 (1977).

24. F. Herlemont, M. Lyszak, J. Lemaire, and J. Demaison, Z. Naturforsch 36a, 944-947 (1981).

25. T. Y. Chang and T. J. Bridges, Opt. Commun. 1, 423-426 (1970).

26. T. Y. Chang and J. D. McGee, Appl. Phys. Lett. 19, 103-105 (1971).

27. E. Bava, A. DeMarchi, A. Godone, R. Benedetti, M. Inguscio, P. Minguzzi, F. Strumia, and M. Tonelli, Opt. Commun. 21, 46-48 (1977).

28. H. E. Radford, F. R. Peterson, D. A. Jennings, and J. A. Mucha, IEEE J. Quantum Electron. QE-13, 92-94 (1977).

29. P. Helminger, J. K. Messer, and F. C. De Lucia, Appl. Phys. Lett. 42, 309-310 (1983).

30. W. C. King and W. Gordy, Phys. Rev. 93, 407-412 (1971).

31. T. Y. Chang: in Reviews of Infrared and Millimeter Waves, 2, 1-28 (Plenum Press, New York 1984).

32. F. R. Petersen, E. C. Beaty, and C. R. Pollock, J. Mol. Spectrosc. 102, 112-122 (1983).

33. C. Freed, L. C. Bradley, and R. G. O'Donnell, IEEE J. Quantum Electron. QE-16, 1195-1206 (1980).

34. B. G. Whitford, K. J. Siemsen, H. D. Riccius, and G. R. Hanes, Opt. Commun. 14, 70-74 (1975).

Table VII.

Comparison of Ground-State Rotational Constants of $^{12}CH_3F$.

Parameter	This Work[a]	This work[b]	Arimondo[c]	Boucher[d]
B_o /MHZ	25536.1499(6)	25536.1490(3)	25536.1492(2)	25536.14951(25)
D_J /kHz	60.2330(36)	60.2250(34)	60.207(8)	60.2186(70)
D_{JK} /kHz	439.5743(312)	439.6323(141)	439.62(3)	439.602(43)
H_J /Hz	-0.0218(68)	-0.0385(85)	-0.026(10)	-0.058(18)
H_{JK} /Hz	1.7518(758)	1.9257(408)	0.95(37)	1.81(13)
H_{KJ} /Hz	21.6679(1921)	21.5915(706)	26.2(34)	21.53(70)

[a]Obtained from fit of frequencies listed in Tables I-IV and those indicated in Table V.

[b]Obtained from fit of the frequencies in Table III.

[c]Obtained from Table 3 (Column 2) in Ref. 5.

[d]Obtained from Table I (MW data only) in Ref. 20.

Figure Captions

1. Block diagram of the infrared laser microwave sideband spectrometer at MSU.

2. Portion of the R(15,K) spectrum in the ν_3 band of $^{12}CH_3F$ recorded with the infrared laser microwave sideband spectrometer. The horizontal axis shows the microwave frequency to be subtracted from the frequency of the 9R(12) CO_2 laser to obtain the spectrometer frequency. The spectrum shown is a composite of two recordings; the sample pressures were ~100 mTorr and ~50 mTorr for the left and right halves, respectively.

3. Portion of the Q(18,K) spectrum in the $2\nu_3 \leftarrow \nu_3$ band of $^{12}CH_3F$ recorded with the infrared laser microwave sideband spectrometer. The horizontal axis shows the microwave frequency to be subtracted from the frequency of the 9P(38) CO_2 laser to obtain the spectrometer frequency. The sample pressure was ~1 Torr.

4. Block diagram of the millimeter/submillimeter wave spectrometer at Duke University.

5. The observed rotational absorption line for the J=12←11, K=2 transition in the v_3=1 state of $^{12}CH_3F$. The sample pressure was ~35 mTorr and the total integration time was ~5 minutes.

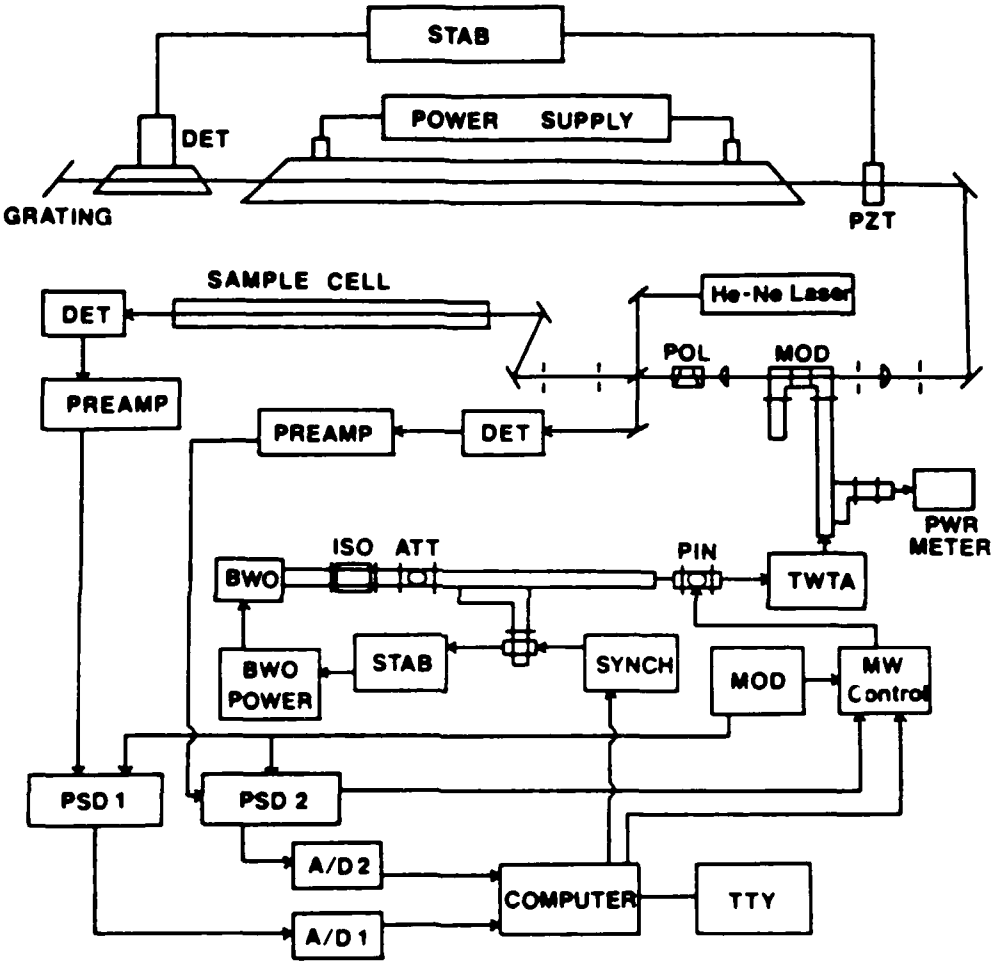
STAB
POWER SUPPLY
DET
GRATING
PZT
SAMPLE CELL
DET
He-Ne Laser
POL
MOD
PREAMP
PREAMP
DET
PWR METER
ISO ATT
PIN
BWO
TWTA
BWO POWER
STAB
SYNCH
MOD
MW Control
PSD 1
PSD 2
A/D 2
COMPUTER
TTY
A/D 1

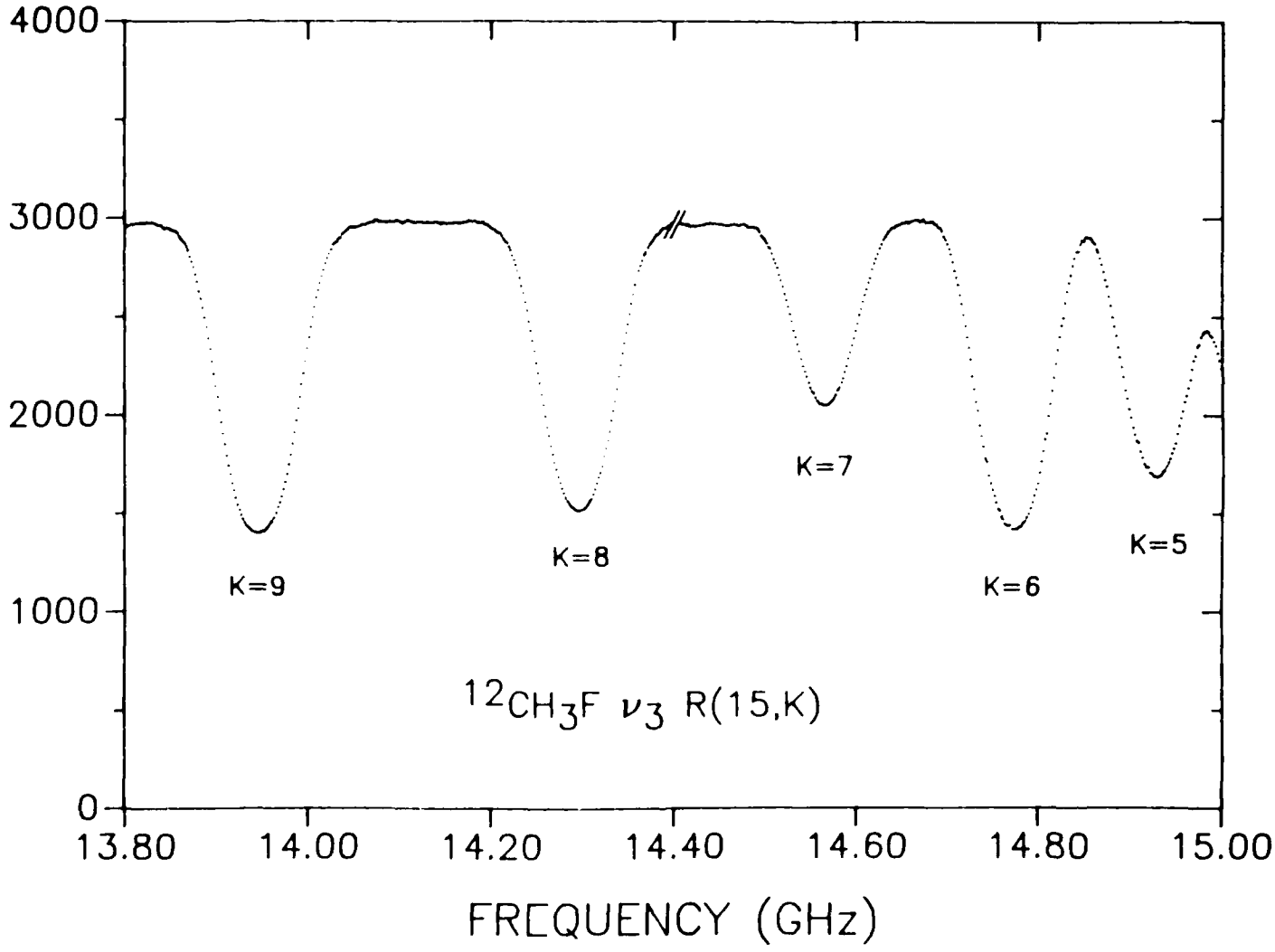
4000
3000
2000
1000
0
K=9
K=8
K=7
K=6
K=5
$^{12}CH_3F$ ν_3 R(15,K)
13.80
14.00
14.20
14.40
14.60
14.80
15.00
FREQUENCY (GHz)

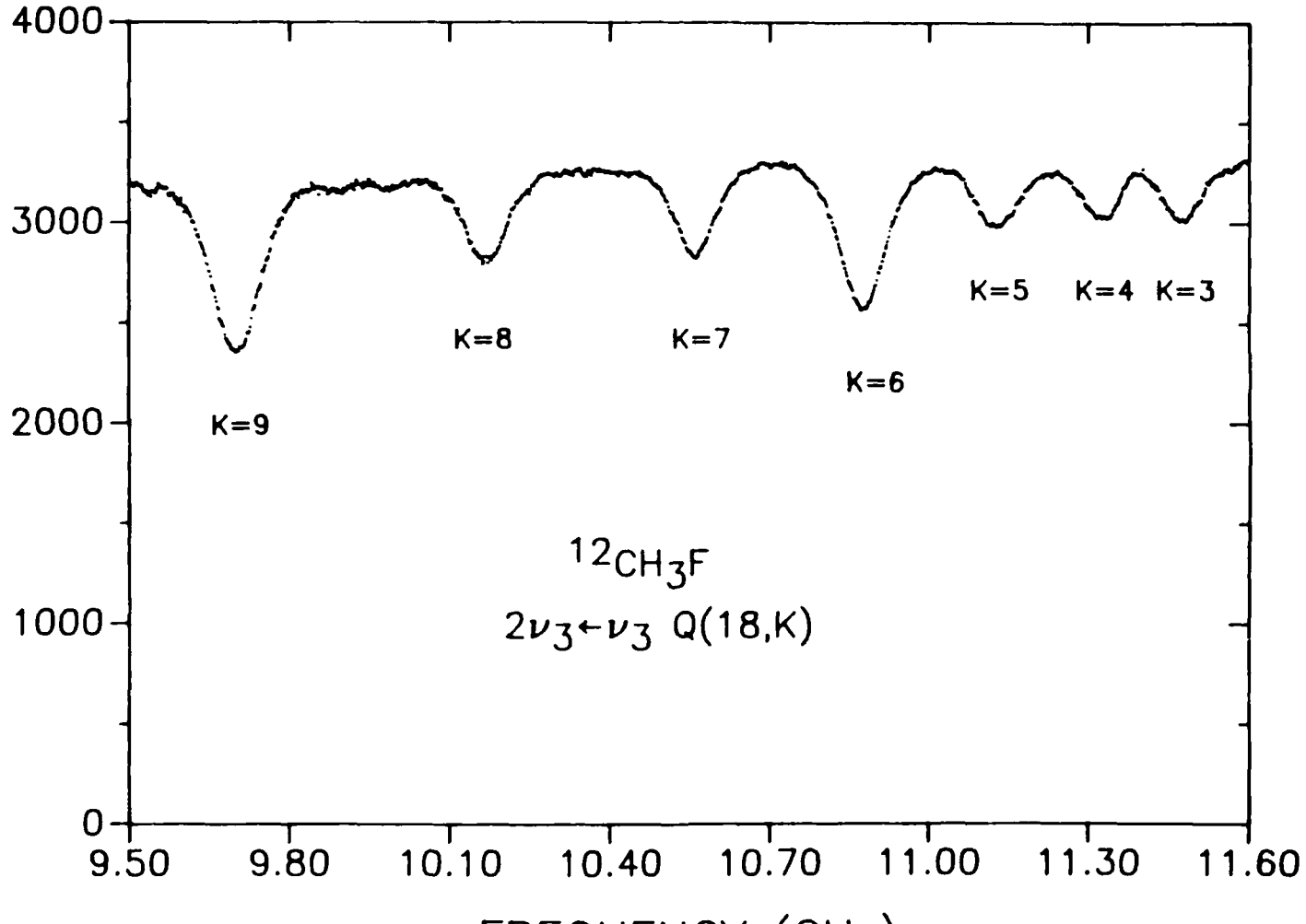
4000
3000
2000
1000
0
K=9
K=8
K=7
K=6
K=5
K=4
K=3
$^{12}CH_3F$
$2\nu_3 \leftarrow \nu_3$ Q(18,K)
9.50
9.80
10.10
10.40
10.70
11.00
11.30
11.60
FREQUENCY (GHz)

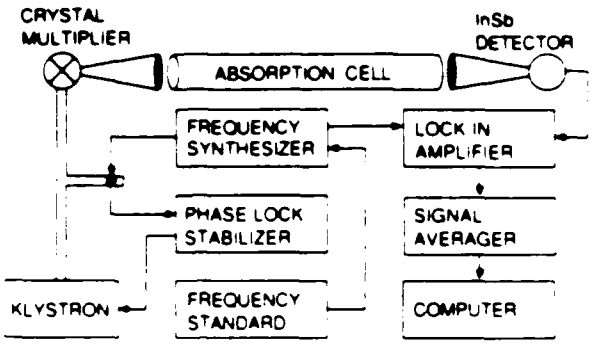
CRYSTAL MULTIPLIER
InSb DETECTOR
ABSORPTION CELL
FREQUENCY SYNTHESIZER
LOCK IN AMPLIFIER
PHASE LOCK STABILIZER
SIGNAL AVERAGER
KLYSTRON
FREQUENCY STANDARD
COMPUTER

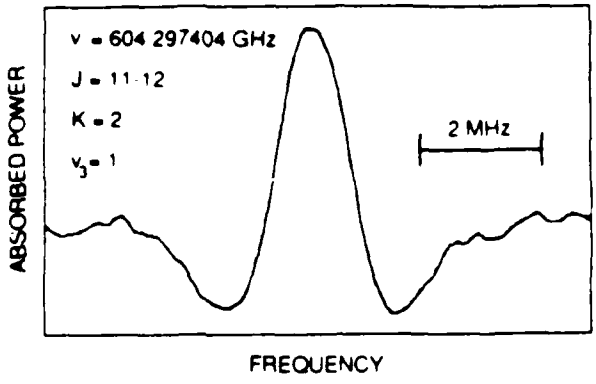
ν = 604 297404 GHz
J = 11-12
K = 2
v_3 = 1
2 MHz
ABSORBED POWER
FREQUENCY

END

3-87

DTIC